Doubly-Robust Self-Training

Anonymous Author(s)
Affiliation
Address
email

Abstract

Self-training is a well-established technique in semi-supervised learning, which leverages unlabeled data by generating pseudo-labels and incorporating them with a limited labeled dataset for training. The effectiveness of self-training heavily relies on the accuracy of these pseudo-labels. In this paper, we introduce doubly-robust self-training, an innovative semi-supervised algorithm that provably balances between two extremes. When pseudo-labels are entirely incorrect, our method reduces to a training process solely using labeled data. Conversely, when pseudo-labels are completely accurate, our method transforms into a training process utilizing all pseudo-labeled data and labeled data, thus increasing the effective sample size. Through empirical evaluations on both the ImageNet dataset for image classification and the nuScenes autonomous driving dataset for 3D object detection, we demonstrate the superiority of the doubly-robust loss over the self-training baseline.

1 Introduction

Semi-supervised learning considers the problem of machine learning given a large unlabeled dataset and a small labeled dataset. It plays an important role in the problem of model finetuning, model distillation, self-training, transfer learning and continual learning (Zhu, 2005; Pan and Yang, 2010; Weiss et al., 2016; Gou et al., 2021; De Lange et al., 2021). To best utilize the unlabeled data, one common assumption in distillation or self-training is that one has access to a teacher model obtained from prior training processes, which may or may not be accurate in the target task due to potential distribution shift. In this paper, we ask the following question:

> Given a teacher model, a large unlabeled dataset and a small labeled dataset, how can we design a principled learning process that ensures consistent and sample-efficient learning of the true model?

One widely adopted and popular approach in computer vision and autonomous driving for leveraging information from all three components is self-training (Lee, 2013; Berthelot et al., 2019b,a; Sohn et al., 2020a; Xie et al., 2020; Jiang et al., 2022; Qi et al., 2021). This approach involves using a teacher model to generate pseudo-labels for all unlabeled data, and then training a new model on a mixture of both pseudo-labeled and labeled data. However, this method can lead to overreliance on the teacher model and can miss important information provided by the labeled data. As a consequence, the self-training approach becomes highly sensitive to the accuracy of the teacher model. Our study demonstrates that even in the simplest scenario of mean estimation, this method can yield significant failures when the teacher model lacks accuracy.

To overcome this issue, we propose an alternative method that is doubly robust. When the covariate distribution of the unlabeled dataset and the labeled dataset matches, the estimator is always consistent no matter whether the teacher model is accurate or not. On the other hand, when the teacher model is an accurate predictor, the estimator makes full use of the pseudo-labeled dataset and greatly increases

Submitted to 37th Conference on Neural Information Processing Systems (NeurIPS 2023). Do not distribute.

the effective sample size. The idea is inspired by and directly related to the missing data inference in the literature of causal inference (Rubin, 1976; Kang and Schafer, 2007; Birhanu et al., 2011; Ding and Li, 2018), the semi-parametric mean estimation (Zhang et al., 2019), and the recent work on prediction-powered inference (Angelopoulos et al., 2023).

1.1 Main Results

The proposed algorithm is a simple modification of the original loss for self-training. Assume that we are given a set of unlabeled samples $\mathcal{D}_1 = \{X_1, X_2, \cdots, X_m\}$, drawn from a fixed distribution $\mathbb{P}_X$, a set of labeled samples $\mathcal{D}_2 = \{(X_{m+1}, Y_{m+1}), (X_{m+2}, Y_{m+2}), \cdots, (X_{m+n}, Y_{m+n})\}$ drawn from some joint distribution $\mathbb{P}_X \times \mathbb{P}_{Y|X}$, and a teacher model $\hat{f}$. Let $\ell_\theta(x, y)$ be a pre-specified loss function that characterizes the prediction error of the estimator with parameter θ on the given sample (X, Y). The traditional self-training aims at minimizing the combined loss for both labeled and unlabeled samples, where the pseudo-labels for unlabeled samples are generated using $\hat{f}$:

$$\mathcal{L}^{\mathsf{SL}}_{\mathcal{D}_1,\mathcal{D}_2}(\theta) = \frac{1}{m+n}\left(\sum_{i=1}^{m} \ell_\theta(X_i, \hat{f}(X_i)) + \sum_{i=m+1}^{m+n} \ell_\theta(X_i, Y_i)\right).$$

Note that it can also be viewed as the first using $\hat{f}$ to predict all the data, and then replace the labeled ones with the known labels.

$$\mathcal{L}^{\mathsf{SL}}_{\mathcal{D}_1,\mathcal{D}_2}(\theta) = \frac{1}{m+n}\sum_{i=1}^{m+n} \ell_\theta(X_i, \hat{f}(X_i)) - \frac{1}{m+n}\sum_{i=m+1}^{m+n} \ell_\theta(X_i, \hat{f}(X_i)) + \frac{1}{m+n}\sum_{i=m+1}^{m+n} \ell_\theta(X_i, Y_i).$$

As an alternative, our proposed doubly robust loss simply replaces the coefficient $1/(m+n)$ with $1/n$ in the last two terms.

$$\mathcal{L}^{\mathsf{DR}}_{\mathcal{D}_1,\mathcal{D}_2}(\theta) = \frac{1}{m+n}\sum_{i=1}^{m+n} \ell_\theta(X_i, \hat{f}(X_i)) - \frac{1}{n}\sum_{i=m+1}^{m+n} \ell_\theta(X_i, \hat{f}(X_i)) + \frac{1}{n}\sum_{i=m+1}^{m+n} \ell_\theta(X_i, Y_i).$$

With such a small change, the estimator becomes consistent and a doubly robust estimator.

Theorem 1 (Informal)**.** *Let $\theta^\star$ be the minimizer of the original loss $\theta^\star = \arg\min_\theta \mathbb{E}_{(X,Y)\sim\mathbb{P}_X\times\mathbb{P}_{Y|X}}[\ell_\theta(X, Y)]$. Under certain regularity conditions, we have*

$$\|\nabla_\theta \mathcal{L}^{\mathsf{DR}}_{\mathcal{D}_1,\mathcal{D}_2}(\theta^\star)\|_2 \lesssim \begin{cases} \sqrt{\frac{d}{m+n}}, & \textit{when } Y \equiv \hat{f}(X), \\ \sqrt{\frac{d}{n}}, & \textit{otherwise}. \end{cases}$$

On the other hand, there exists instances such that $\|\nabla_\theta \mathcal{L}^{\mathsf{SL}}_{\mathcal{D}_1,\mathcal{D}_2}(\theta^\star)\|_2 \geq C$ always holds true no matter how large m, n are.

The result shows that the true parameter $\theta^\star$ is also a local minimum of the doubly-robust loss, but not a local minimum of the original self-training loss. We also provide more detailed comparisons for the special example of mean estimation in Section 2.2, and the empirical results on image and driving datasets are provided in Section 3.

1.2 Related Work

Missing Data Inference and Causal Inference. The problem of missing data inference has been a central and fundamental problem in causal inference. For each unit in the experiment, at most one of the potential outcomes—the one corresponding to the treatment to which the unit is exposed—is observed, and the other potential outcomes are missing (Holland, 1986; Ding and Li, 2018). The doubly robust method combines the virtues of data imputation Rubin (1979) and propensity score weighting Rosenbaum and Rubin (1983). The estimator is named doubly robust due to the following property: if the model for imputation is correctly specified then it is consistent no matter whether the propensity score model is correctly specified; on the other hand, if the model propensity score model is correctly specified, then it is consistent no matter whether the model for imputation is correctly specified (Scharfstein et al., 1999; Bang and Robins, 2005; Birhanu et al., 2011; Ding and Li, 2018).

Another line of work that is also inspired by the doubly robust estimator in causal inference is double machine learning (Semenova et al., 2017; Chernozhukov et al., 2018a,b; Foster and Syrgkanis, 2019). The problem in double machine learning is related to the classic semi-parametric problem of inference on a low-dimensional parameter in the presence of high-dimensional nuisance parameters, and thus is different from our question of semi-supervised learning.

Self-Training. Self-training is a popular semi-supervised learning paradigm in which machine-generated pseudo-labels are used for training with unlabeled data (Lee, 2013; Berthelot et al., 2019b,a; Sohn et al., 2020a). To generate these pseudo-labels, a teacher model is pre-trained on a set of labeled data, and its predictions on the unlabeled data are extracted as pseudo-labels. Previous work seeks to address the noisy quality of pseudo-labels in various ways. MixMatch Berthelot et al. (2019b) ensembles pseudo-labels across several augmented views of the input data. ReMixMatch Berthelot et al. (2019a) extends this by weakly augmenting the teacher inputs and strongly augmenting the student inputs. FixMatch Sohn et al. (2020a) uses confidence thresholding to select only high-quality pseudo-labels for student training.

Self-training has been applied in both 2D (Liu et al., 2021a; Jeong et al., 2019; Tang et al., 2021; Sohn et al., 2020b; Zhou et al., 2022) and 3D (Park et al., 2022; Wang et al., 2021; Li et al., 2023; Liu et al., 2023) object detection. STAC Sohn et al. (2020b) enforces consistency between strongly augmented versions of confidence-filtered pseudo-labels. Unbiased teacher Liu et al. (2021a) updates the teacher during training with an exponential moving average (EMA) of the student network weights. Dense Pseudo-Label Zhou et al. (2022) replaces box pseudo-labels with the raw output features of the detector to allow the student to learn richer context. In the 3D domain, 3DIoUMatch Wang et al. (2021) thresholds pseudo-labels using a model-predicted Intersection-over-Union (IoU). DetMatch Park et al. (2022) performs detection in both the 2D and 3D domains and filters pseudo-labels based on 2D-3D correspondence. HSSDA Liu et al. (2023) extends strong augmentation during training with a patch-based point cloud shuffling augmentation. Offboard3D Qi et al. (2021) utilizes multiple frames of temporal context to improve pseudo-label quality.

There have been some theoretical analyses for the case of semi-supervised inference for mean estimation and linear regression (Zhang et al., 2019; Azriel et al., 2022). Our analysis bridges the gap between these approaches and the doubly-robust estimators in causal inference literature. Our proposed loss can be viewed as a generalization of these approaches, and can exactly reduce to the same estimator when considering mean estimation.

2 Doubly-Robust Self-Training

2.1 Proposed Algorithm

We begin with the case where the marginal distributions of the covariate of the labeled and unlabeled datasets are the same. Assume that we are given a set of unlabeled samples $\mathcal{D}_1 = \{X_1, X_2, \cdots, X_m\}$, drawn from a fixed distribution $\mathbb{P}_X$ supported on $\mathcal{X}$, a set of labeled samples $\mathcal{D}_2 = \{(X_{m+1}, Y_{m+1}), (X_{m+2}, Y_{m+2}), \cdots, (X_{m+n}, Y_{m+n})\}$ drawn from some joint distribution $\mathbb{P}_X \times \mathbb{P}_{Y|X}$ supported on $\mathcal{X} \times \mathcal{Y}$, and a pre-trained model $\hat{f} : \mathcal{X} \mapsto \mathcal{Y}$. Let $\ell_\theta(\cdot, \cdot) : \mathcal{X} \times \mathcal{Y} \mapsto \mathbb{R}$ be a pre-specified loss function that characterizes the prediction error of the estimator with parameter θ on the given sample (X, Y). Our target is to find some $\theta^\star \in \Theta$ that satisfies

$$\theta^\star \in \arg\min_{\theta \in \Theta} \mathbb{E}_{(X,Y)\sim \mathbb{P}_X \times \mathbb{P}_{Y|X}}[\ell_\theta(X, Y)].$$

For any loss $\ell_\theta(x, y)$, consider the first simple estimator which ignores the predictor $\hat{f}$ and only trains on the labeled samples:

$$\mathcal{L}^{\mathsf{TL}}_{\mathcal{D}_1,\mathcal{D}_2}(\theta) = \frac{1}{n} \sum_{i=m+1}^{m+n} \ell_\theta(X_i, Y_i).$$

This can be a safe choice since it's always an empirical risk minimizer. As $n \to \infty$, the loss converges to the population loss. However, it ignores all the information provided in $\hat{f}$ and the unlabeled dataset, which makes it less sample efficient when the predictor $\hat{f}$ is informative.

On the other hand, the traditional self-training aims at minimizing the combined loss for both labeled and unlabeled samples, where the pseudo-labels for unlabeled samples are generated using $\hat{f}$[1]:

$$\begin{aligned}\mathcal{L}^{\mathsf{SL}}_{\mathcal{D}_1,\mathcal{D}_2}(\theta) &= \frac{1}{m+n}\left(\sum_{i=1}^{m}\ell_\theta(X_i,\hat{f}(X_i)) + \sum_{i=m+1}^{m+n}\ell_\theta(X_i,Y_i)\right)\\ &= \frac{1}{m+n}\sum_{i=1}^{m+n}\ell_\theta(X_i,\hat{f}(X_i)) - \frac{1}{m+n}\sum_{i=m+1}^{m+n}\ell_\theta(X_i,\hat{f}(X_i)) + \frac{1}{m+n}\sum_{i=m+1}^{m+n}\ell_\theta(X_i,Y_i).\end{aligned}$$

As is shown by the last equality, the self-training loss can be viewed as first using $\hat{f}$ to predict all the samples (including the labeled samples) and computing the average loss, then replacing part of the loss for labeled samples with the loss on provided labels. Although the loss uses the information of the unlabeled samples and $\hat{f}$, the performance can be bad when the predictor is not accurate.

On the other hand, we propose an alternative loss, which simply replaces the weight $1/(m+n)$ in the last two terms with $1/n$:

$$\mathcal{L}^{\mathsf{DR}}_{\mathcal{D}_1,\mathcal{D}_2}(\theta) = \frac{1}{m+n}\sum_{i=1}^{m+n}\ell_\theta(X_i,\hat{f}(X_i)) - \frac{1}{n}\sum_{i=m+1}^{m+n}\ell_\theta(X_i,\hat{f}(X_i)) + \frac{1}{n}\sum_{i=m+1}^{m+n}\ell_\theta(X_i,Y_i). \quad (1)$$

As we will show later, this is a doubly-robust estimator. We provide an intuitive interpretation here:

- In the case when the given predictor is always accurate, i.e. $\hat{f}(X) \equiv Y$ always holds (which also means that $Y|X=x$ is a deterministic function of x), the last two terms cancel, and the loss is exactly minimizing the average loss $\frac{1}{m+n}\sum_{i=1}^{m+n}\ell_\theta(X_i,\hat{f}(X_i))$ on all the data provided. The effective sample size is $m+n$, compared with effective sample size n for training only on labeled dataset $\mathcal{L}^{\mathsf{TL}}$. In this case, the loss $\mathcal{L}^{\mathsf{DR}}$ is much better than $\mathcal{L}^{\mathsf{TL}}$, and comparable to $\mathcal{L}^{\mathsf{SL}}$.

  We may as well relax the assumption of $\hat{f}(X) = Y$ to $\mathbb{E}[\ell_\theta(X,\hat{f}(X))] = \mathbb{E}[\ell_\theta(X,Y)]$. As n grows larger, the loss is approximately minimizing the average loss $\frac{1}{m+n}\sum_{i=1}^{m+n}\ell_\theta(X_i,\hat{f}(X_i))$.
- On the other hand, no matter how bad the given predictor is, the difference between the first two terms vanishes as either of m,n goes to infinity since the labeled samples $X_{m+1},\cdots,X_{m+n}$ follow the same distribution as $X_1,\cdots,X_m$. Thus asymptotically the loss is minimizing $\frac{1}{n}\sum_{i=m+1}^{m+n}\ell_\theta(X_i,Y_i)$, which discards the bad predictor $\hat{f}$ and only focuses on the labeled dataset. Thus in this case, the loss $\mathcal{L}^{\mathsf{DR}}$ is much better than $\mathcal{L}^{\mathsf{SL}}$, and comparable to $\mathcal{L}^{\mathsf{TL}}$.

This loss shall only be used when the covariate distributions between labeled and unlabeled samples match. In the case where there is a distribution mismatch, we propose an alternative loss in Section 2.4. A similar idea is also proposed in Angelopoulos et al. (2023) for constructing the confidence interval with a given teacher model. However, they focus on the case where the teacher model is accurate to tighten the confidence interval, while we focus on the doubly-robust property of the estimator.

2.2 Motivating example: mean estimation

As a concrete example, in the case of one-dimensional mean estimation we can take $\ell_\theta(X,Y) = (\theta - Y)^2$. Our target is to find some $\theta^\star$ that satisfies

$$\theta^\star = \arg\min_\theta \mathbb{E}_{(X,Y)\sim\mathbb{P}_X\times\mathbb{P}_{Y|X}}[(\theta-Y)^2].$$

One can see that $\theta^\star = \mathbb{E}[Y]$. In this case, the loss for training only on labeled data becomes

$$\mathcal{L}^{\mathsf{TL}}_{\mathcal{D}_1,\mathcal{D}_2}(\theta) = \frac{1}{n}\sum_{i=m+1}^{m+n}(\theta - Y_i)^2.$$

[1]There are several variants of the traditional self-training loss. For example, Xie et al. (2020) introduces an extra weight $(m+n)/n$ on the labeled samples, and adds noise to the student model; Sohn et al. (2020a) uses confidence thresholding to filter unreliable pseudo-labels. However, both of the alternatives still suffer from the inconsistency issue. In this paper we focus on the simplest form $\mathcal{L}^{\mathsf{SL}}$.

And the optimal parameter is $\hat{\theta}_{\mathsf{TL}} = \frac{1}{n}\sum_{i=m+1}^{m+n} Y_i$, which is a simple empirical average over all observed Y's.

For a given pre-existing predictor $\hat{f}$, the loss for self-training becomes

$$\mathcal{L}^{\mathsf{SL}}_{\mathcal{D}_1,\mathcal{D}_2}(\theta) = \frac{1}{m+n}\left(\sum_{i=1}^{m}(\theta - \hat{f}(X_i))^2 + \sum_{i=m+1}^{m+n}(\theta - Y_i)^2\right)$$

It's straightforward to see that the minimizer of the loss is the unweighted average between the unlabeled predictors $\hat{f}(X_i)$'s and the labeled Y_i's, i.e.

$$\theta^\star_{\mathsf{SL}} = \frac{1}{m+n}\left(\sum_{i=1}^{m}\hat{f}(X_i) + \sum_{i=m+1}^{m+n} Y_i\right).$$

In the case of $m \gg n$, the mean estimator is almost the same as the average of all the predicted value on the unlabeled dataset, which can be far from $\theta^\star$ when the predictor $\hat{f}$ is inaccurate.

On the other hand, for the proposed doubly robust estimator, we have

$$\begin{aligned}\mathcal{L}^{\mathsf{DR}}_{\mathcal{D}_1,\mathcal{D}_2}(\theta) &= \frac{1}{m+n}\sum_{i=1}^{m+n}(\theta - \hat{f}(X_i))^2 - \frac{1}{n}\sum_{i=m+1}^{m+n}(\theta - \hat{f}(X_i))^2 + \frac{1}{n}\sum_{i=m+1}^{m+n}(\theta - Y_i)^2 \\ &= \frac{1}{m+n}\sum_{i=1}^{m+n}(\theta - \hat{f}(X_i))^2 + \frac{1}{n}\sum_{i=m+1}^{m+n} 2(\hat{f}(X_i) - Y_i)\theta + Y_i^2 - \hat{f}(X_i)^2.\end{aligned}$$

Note that the loss is still convex, and we have

$$\theta^\star_{\mathsf{DR}} = \frac{1}{m+n}\sum_{i=1}^{m+n}\hat{f}(X_i) - \frac{1}{n}\sum_{i=m+1}^{m+n}(\hat{f}(X_i) - Y_i).$$

This recovers the estimator in prediction-powered inference (Angelopoulos et al., 2023). Assume that $\hat{f}$ is independent of the labeled data. We can calculate the mean squared error of the three estimators as follows.

Proposition 1. *Let* $\mathsf{Var}[\hat{f}(X) - Y] = \mathbb{E}[(\hat{f}(X) - Y)^2 - \mathbb{E}[(\hat{f}(X) - Y)]^2]$. *We have*

$$\mathbb{E}[(\theta^\star - \hat{\theta}_{\mathsf{TL}})^2] = \frac{1}{n}\mathsf{Var}[Y],$$

$$\mathbb{E}[(\theta^\star - \hat{\theta}_{\mathsf{SL}})^2] \le \frac{2m^2}{(m+n)^2}\mathbb{E}[(\hat{f}(X) - Y)]^2 + \frac{2m}{(m+n)^2}\mathsf{Var}[\hat{f}(X) - Y] + \frac{2n}{(m+n)^2}\mathsf{Var}[Y],$$

$$\mathbb{E}[(\theta^\star - \hat{\theta}_{\mathsf{DR}})^2] \le 2\min\left(\frac{1}{n}\mathsf{Var}[Y] + \frac{m+2n}{(m+n)n}\mathsf{Var}[\hat{f}(X)], \frac{m+2n}{(m+n)n}\mathsf{Var}[\hat{f}(X) - Y] + \frac{1}{m+n}\mathsf{Var}[Y]\right).$$

The proof is deferred to Appendix E. From the proposition, we can see the double-robustness of $\hat{\theta}_{\mathsf{DR}}$: no matter how bad estimator $\hat{f}(X)$ is, the rate is always upper bounded by $\frac{4}{n}(\mathsf{Var}[Y] + \mathsf{Var}[\hat{f}(X)])$. On the other hand, when $\hat{f}(X)$ is accurate estimator of Y (i.e. $\mathsf{Var}[\hat{f}(X) - Y]$ is small), the rate can be improved to $\frac{2}{m+n}\mathsf{Var}[Y]$. In contrast, the self-training loss always has a non-vanishing term $\frac{2m^2}{(m+n)^2}\mathbb{E}[(\hat{f}(X) - Y)]^2$ when $m \gg n$, unless the predictor $\hat{f}$ is accurate.

On the other hand, when $\hat{f}(x) = \hat{\beta}_{(-1)}^\top x + \hat{\beta}_1$ is a linear predictor trained on the labeled data with $\hat{\beta} = \arg\min_{\beta=[\beta_1,\beta_{(-1)}]}\frac{1}{n}\sum_{i=m+1}^{m+n}(\beta_{(-1)}^\top X_i + \beta_1 - Y_i)^2$, our estimator reduces to the estimator in the semi-supervised mean estimator in Zhang et al. (2019). Let $\tilde{X} = [1, X]$. We have the following result that reveals the superiority of the doubly robust estimator compared to the other two options.

Proposition 2 ((Zhang et al., 2019))**.** *We provide the asymptotic behavior when* $\hat{f}$ *is a linear predictor trained on the labeled data:*

- *Self-training* $\hat{\theta}_{\mathsf{SL}}$ *is biased and thus inconsistent:*

$$\mathbb{E}[\hat{\theta}_{\mathsf{DR}} - \theta^\star] = \frac{m}{m+n}\mathbb{E}[\beta^\top\tilde{X} - Y]$$

- *Training only on labeled data $\hat{\theta}_{\mathsf{TL}}$ is unbiased but large variance:*
$$\sqrt{n}(\hat{\theta}_{\mathsf{TL}} - \theta^\star) \to \mathcal{N}(0, \mathbb{E}[(Y - \beta^\top \tilde{X})^2] + \beta_{(-1)}^\top \Sigma \beta_{(-1)})$$

- *Doubly Robust $\hat{\theta}_{\mathsf{DR}}$ is unbiased with smaller variance:*
$$\sqrt{n}(\hat{\theta}_{\mathsf{DR}} - \theta^\star) \to \mathcal{N}(0, \mathbb{E}[(Y - \beta^\top \tilde{X})^2] + \frac{n}{m+n}\beta_{(-1)}^\top \Sigma \beta_{(-1)})$$

Here $\beta = \arg\min_\beta \mathbb{E}[(Y - \beta^\top \tilde{X})^2]$, $\Sigma = \mathbb{E}[(X - \mathbb{E}[X])(X - \mathbb{E}[X])^\top]$.

2.3 Guarantee for general loss

In the general case, we show that the doubly robust loss function still provides a good landscape. In particular, as n, m goes to infinity, the global minimum of the original loss is also a critical point of the new doubly robust loss, no matter how bad the predictor $\hat{f}$ is.

Let $\theta^\star$ be the minimizer of $\mathbb{E}_{\mathbb{P}_{X,Y}}[\ell_\theta(X, Y)]$. Let $\hat{f}$ be a pre-existing model that does not depend on the dataset $\mathcal{D}_1, \mathcal{D}_2$. We also make the following regularity assumptions.

Assumption 1. *The loss $\ell_\theta(x, y)$ is differentiable at $\theta^\star$ for any x, y.*

Assumption 2. *The random variables $\nabla_\theta \ell_\theta(X, \hat{f}(X))$ and $\nabla_\theta \ell_\theta(X, Y)$ have bounded first and second moments.*

With this assumption, we denote $\Sigma_\theta^{Y-\hat{f}} = \mathsf{Cov}[\nabla_\theta \ell_\theta(X, \hat{f}(X)) - \nabla_\theta \ell_\theta(X, Y)]$, $\Sigma_\theta^{\hat{f}} = \mathsf{Cov}[\nabla_\theta \ell_\theta(X, \hat{f}(X))]$, $\Sigma_\theta^{Y} = \mathsf{Cov}[\nabla_\theta \ell_\theta(X, Y)]$.

Theorem 2. *Under Assumption 1 and 2, we have that with probability at least $1 - \delta$,*

$$\begin{aligned}\|\nabla_\theta \mathcal{L}^{\mathsf{DR}}_{\mathcal{D}_1,\mathcal{D}_2}(\theta^\star)\|_2 \leq & C \min\Bigg(\|\Sigma_{\theta^\star}^{\hat{f}}\|_2 \sqrt{\frac{d}{(m+n)\delta}} + \|\Sigma_{\theta^\star}^{Y-\hat{f}}\|_2 \sqrt{\frac{d}{n\delta}}, \\ & \|\Sigma_{\theta^\star}^{\hat{f}}\|_2 \left(\sqrt{\frac{d}{(m+n)\delta}} + \sqrt{\frac{d}{n\delta}} \right) + \|\Sigma_{\theta^\star}^{Y}\|_2 \sqrt{\frac{d}{n\delta}} \Bigg).\end{aligned}$$

Here C is some universal constant, and $\mathcal{L}^{\mathsf{DR}}_{\mathcal{D}_1,\mathcal{D}_2}$ is defined in Equation (1).

The proof is deferred to Appendix F. From the example of mean estimation we know that one can design instances such that $\|\nabla_\theta \mathcal{L}^{\mathsf{SL}}_{\mathcal{D}_1,\mathcal{D}_2}(\theta^\star)\|_2 \geq C$ for some positive constant C.

When the loss $\nabla_\theta \mathcal{L}^{\mathsf{DR}}_{\mathcal{D}_1,\mathcal{D}_2}$ is convex, it implies that the global minimum of $\nabla_\theta \mathcal{L}^{\mathsf{DR}}_{\mathcal{D}_1,\mathcal{D}_2}$ converges to $\theta^\star$ as both m, n go to infinity. When the loss $\nabla_\theta \mathcal{L}^{\mathsf{DR}}_{\mathcal{D}_1,\mathcal{D}_2}$ is strongly convex, it also implies that $\|\hat{\theta} - \theta^\star\|_2$ converges to 0 as both m, n go to infinity, where $\hat{\theta}$ is the minimizer of $\nabla_\theta \mathcal{L}^{\mathsf{DR}}_{\mathcal{D}_1,\mathcal{D}_2}$.

When $\hat{f}$ is a perfect predictor with $\hat{f}(X) \equiv Y$ (and $Y|X = x$ is deterministic), one has $\mathcal{L}^{\mathsf{DR}}_{\mathcal{D}_1,\mathcal{D}_2}(\theta^\star) = \frac{1}{m+n}\sum_{i=1}^{m+n} \ell_\theta(X_i, Y_i)$. The effective sample size is $m + n$ instead of n in $\mathcal{L}^{\mathsf{SL}}_{\mathcal{D}_1,\mathcal{D}_2}(\theta)$.

When $\hat{f}$ is also trained from the labeled data, one may apply data splitting to achieve the same guarantee up to a constant factor. We provide more discussions in Appendix D.

2.4 The case of distribution mismatch

We also consider the case where the marginal distributions of the covariate of the labeled and unlabeled datasets are different. Assume that we are given a set of unlabeled samples $\mathcal{D}_1 = \{X_1, X_2, \cdots, X_m\}$, drawn from a fixed distribution $\mathbb{P}_X$, a set of labeled samples $\mathcal{D}_2 = \{(X_{m+1}, Y_{m+1}), (X_{m+2}, Y_{m+2}), \cdots, (X_{m+n}, Y_{m+n})\}$ drawn from some joint distribution $\mathbb{Q}_X \times \mathbb{P}_{Y|X}$, and a pre-trained model $\hat{f}$. In the case when the labeled samples do not follow the same distribution as the unlabeled samples, we may need to introduce the importance weight $\pi(x)$. This introduces the following doubly robust estimator:

$$\mathcal{L}^{\mathsf{DR2}}_{\mathcal{D}_1,\mathcal{D}_2}(\theta) = \frac{1}{m}\sum_{i=1}^{m} \ell_\theta(X_i, \hat{f}(X_i)) - \frac{1}{n}\sum_{i=m+1}^{m+n} \frac{1}{\pi(X_i)} \ell_\theta(X_i, \hat{f}(X_i)) + \frac{1}{n}\sum_{i=m+1}^{m+n} \frac{1}{\pi(X_i)} \ell_\theta(X_i, Y_i).$$

Note that we not only introduce the extra importance weight π, but also change the first term from the average of all the $m+n$ samples to the average of n samples.

Proposition 3. *We have* $\mathbb{E}[\mathcal{L}^{\mathsf{DR2}}_{\mathcal{D}_1,\mathcal{D}_2}(\theta)] = \mathbb{E}_{\mathbb{P}_{X,Y}}[\ell_\theta(X,Y)]$ *as long as one of the following two assumptions hold:*

- *For any* x, $\pi(x) = \frac{\mathbb{P}_X(x)}{\mathbb{Q}_X(x)}$.
- *For any* x, $\ell_\theta(x, \hat{f}(x)) = \mathbb{E}_{Y\sim\mathbb{P}_{Y|X=x}}[\ell_\theta(x,Y)]$.

The proof is deferred to Appendix G. The proposition implies that as long as one of the π or $\hat{f}$ is accurate, the expectation of the loss is the same as that of the target loss. When the distributions between unlabeled and labeled samples match each other, it reduces to the case in the previous sections. In this case, taking $\pi(x) = 1$ guarantees that the expectation of the doubly-robust loss is always the same as that of the target loss.

3 Experiments

3.1 Optimization of the Doubly Robust Loss

In practice, we train a neural network with mini-batched stochastic gradient descent. Although we have shown in Theorem 2 that the true parameter remains a local minimum of the doubly robust loss, the optimization landscape might be completely different for the new doubly robust loss. We observed in the experiments that directly minimizing the doubly robust loss in Equation (1) leads to instability. Instead, we propose to minimize the curriculum-based loss in each epoch:

$$\mathcal{L}^{\mathsf{DR},t}_{\mathcal{D}_1,\mathcal{D}_2}(\theta) = \frac{1}{m+n}\sum_{i=1}^{m+n}\ell_\theta(X_i,\hat{f}(X_i)) - \alpha_t\cdot\left(\frac{1}{n}\sum_{i=m+1}^{m+n}\ell_\theta(X_i,\hat{f}(X_i)) - \frac{1}{n}\sum_{i=m+1}^{m+n}\ell_\theta(X_i,Y_i)\right).$$

Here we set $\alpha_t = t/T$, where T is the total number of epochs. For object detection experiments, we introduce the labeled samples only in the final epoch, setting $\alpha_t = 0$ for all epochs before setting $\alpha_t = 1$ in the final epoch. Intuitively, we start from the training with samples only from the pseudo-labels, and gradually introduce the labeled samples in doubly robust loss for fine-tuning. We observe that this greatly stabilizes the training landscape in the experiments below.

3.2 Image Classification

Datasets and Settings. We evaluate our doubly-robust self-training on the ImageNet100 dataset, which contains random 100 classes from ImageNet-1k (Russakovsky et al., 2015), with a number of 120K training images (approximately 1,200 samples per class) and 5,000 validation images (50 samples per class). To further test the effectiveness of our algorithm in a low-data scenario, we create an additional dataset called mini-ImageNet100 by randomly sampling 100 images per class from ImageNet100. Two carefully-selected models are evaluated: **1)** DaViT-T (Ding et al., 2022), a popular vision transformer architecture with state-of-the-art performance on ImageNet, and **2)** ResNet50 (He et al., 2016), a classic and powerful convolutional network to verify the generality of our algorithm.

Baselines. In addition to doubly-robust self-training, we establish 3 baselines: **1)** 'Labeled Only' for training on labeled data only (partial training set) with a loss $\mathcal{L}^{\mathsf{TL}}$, **2)** 'Pseudo Only' for training with pseudo labels generated for all training samples, **3)** 'Labeled + Pseudo' for a mixture of pseudo-labels and labeled data, with the loss $\mathcal{L}^{\mathsf{SL}}$. See **Appendix** for more implementation details and ablations.

Results on ImageNet100. We first conduct experiments on ImageNet100 by training the model for 20 epochs using different fractions of labeled data from 1% to 100%. From the results shown in Fig. 1, we observe that: **1)** Our model outperforms all baseline methods on both two networks by large margins. For example, we achieve 5.5% and 5.3% gains (Top-1 Acc) on DaViT over the 'Labeled + Pseudo' method for 20% and 80% labeled data, respectively. **2)** The 'Labeled + Pseudo' method consistently beats the 'Labeled Only' baseline. **3)** While 'Pseudo Only' works for smaller fractions of the labeled data (less than 30%) on DaViT, it is inferior to 'Labeled Only' on ResNet50.

Results on mini-ImageNet100. We also perform comparisons on mini-ImageNet100 to demonstrate the performance when the total data volume is limited. From the results in Table 1, we see our model

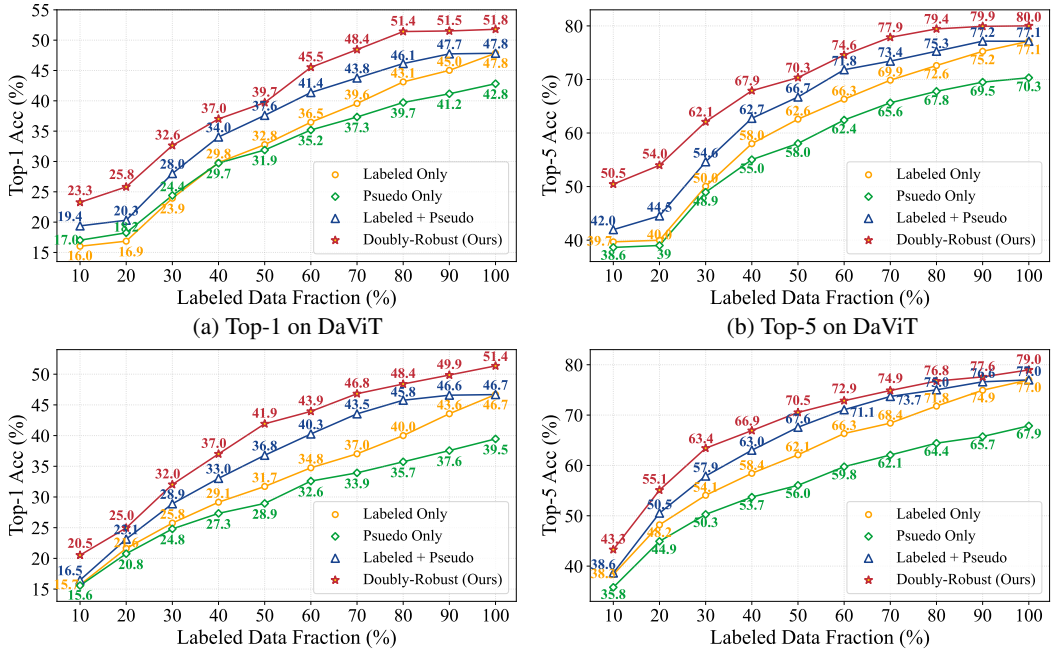

(a) Top-1 on DaViT (b) Top-5 on DaViT

(c) Top-1 on ResNet50 (d) Top-5 on ResNet50

Figure 1: Comparisons on ImageNet100 using two different network architectures. Both Top-1 and Top-5 accuracies are reported. All models are trained for 20 epochs.

Table 1: Comparisons on mini-ImageNet100, all models trained for 100 epochs.

Labeled Data Percent	Labeled Only		Pseudo Only		Labeled + Pseudo		Doubly-Robust Loss	
	top1	top5	top1	top5	top1	top5	top1	top5
1	2.72	9.18	**2.81**	9.57	2.73	9.55	2.75	**9.73**
5	3.92	13.34	4.27	13.66	4.27	14.4	**4.89**	**16.38**
10	6.76	20.84	7.27	21.64	7.65	22.48	**8.01**	**21.90**
20	12.3	31.3	13.46	30.79	**13.94**	**32.63**	13.50	32.17
50	20.69	46.86	20.92	45.2	24.9	50.77	**25.31**	**51.61**
80	27.37	55.57	25.57	50.85	30.63	58.85	**30.75**	**59.41**
100	31.07	60.62	28.95	55.35	**34.33**	62.78	34.01	**63.04**

generally outperforms all baselines. As the dataset size decreases and the number of training epochs increases, the gain of our algorithm becomes smaller. This is expected, as **1)** the models are not adequately trained and thus have noise issues, and **2)** there are insufficient ground truths to compute the last term of our loss function. In extreme cases, there is only 1 labeled sample (1%) per class.

3.3 3D Object Detection

Doubly-Robust Object Detection. Given some visual representation of a scene, 3D object detection aims to generate a set of 3D bounding box predictions $\{b_i\}_{i\in[m+n]}$ and a set of corresponding class predictions $\{c_i\}_{i\in[m+n]}$. Thus, each single ground-truth annotation $Y_i \in Y$ is a set $Y_i = (b_i, c_i)$ containing a box and a class. During training, the object detector is supervised with a sum of the box regression loss $\mathcal{L}_{loc}$ and the classification loss $\mathcal{L}_{cls}$, i.e. $\mathcal{L}_{obj} = \mathcal{L}_{loc} + \mathcal{L}_{cls}$.

In the self-training for object detection, pseudo-labels for a given scene X_i are selected from the labeler predictions $f(X_i)$ based on some user-defined criteria (typically the model's detection confidence). Unlike in standard classification or regression, Y_i will contain a differing number of labels depending on the number of objects in the scene. Furthermore, the number of extracted pseudo-labels $f(X_i)$ will generally not be equal to the number of scene ground-truth labels Y_i due to false positive/negative detections. Therefore it makes sense to express the doubly-robust loss function in terms of the individual box labels as opposed to the scene-level labels. We define the doubly-robust

Table 2: Performance comparison on nuScenes *val* set.

Labeled Data Fraction	Labeled Only		Labeled + Pseudo		Doubly-Robust Loss	
	mAP↑	NDS↑	mAP↑	NDS↑	mAP↑	NDS↑
1/24	7.56	18.01	7.60	17.32	**8.18**	**18.33**
1/16	11.15	20.55	11.60	21.03	**12.30**	**22.10**
1/4	25.66	41.41	**28.36**	**43.88**	27.48	43.18

Table 3: Per-class mAP (%) comparison on nuScenes *val* set using 1/16 of total labels in training.

	Car	Ped	Truck	Bus	Trailer	Barrier	Traffic Cone
Labeled Only	48.6	30.6	8.5	6.2	4.0	6.8	4.4
Labeled + Pseudo	48.8	30.9	8.8	7.5	5.7	6.7	4.0
Improvement	+0.2	+0.3	+0.3	+1.3	**+1.7**	-0.1	-0.4
Doubly-Robust Loss	51.5	32.9	9.6	8.2	5.2	7.2	4.5
Improvement	**+2.9**	**+2.3**	**+1.1**	**+2.0**	+1.2	**+0.4**	**+0.1**

object detection loss as follows:

$$\mathcal{L}_{obj}^{\mathsf{DR}}(\theta) = \frac{1}{M+N_{ps}} \sum_{i=1}^{M+N_{ps}} \ell_\theta(X_i, f(X_i)) - \frac{1}{N_{ps}} \sum_{i=M+1}^{M+N_{ps}} \ell_\theta(X_i', f(X_i')) + \frac{1}{N} \sum_{i=M+1}^{M+N} \ell_\theta(X_i, Y_i).$$

where M is the total number of pseudo-label boxes from the unlabeled split, N is the total number of labeled boxes, X_i' is the scene with pseudo-label boxes from the *labeled* split, and N_{ps} is the total number of pseudo-label boxes from the *labeled* split. We note that the last two terms now contain summations over a differing number of boxes, an upshot of the discrepancy between the number of manually-labeled boxes and pseudo-labeled boxes. Both components of the object detection loss (localization/classification) adopt this form of doubly-robust loss.

Dataset and Setting. To evaluate doubly-robust self-training in the autonomous driving setting, we perform experiments on the large-scale 3D detection dataset nuScenes Caesar et al. (2020). nuScenes is comprised of 1000 scenes (700 training, 150 validation and 150 test) with each frame containing sensor information from RGB camera, LiDAR, and radar scans. Box annotations are comprised of 10 classes, with the class instance distribution following a long-tailed distribution, allowing us to investigate our self-training approach for both common and rare classes. The main 3D detection metrics for nuScenes are mean Average Precision (mAP) and the nuScenes Detection Score (NDS), a dataset-specific metric consisting of a weighted average of mAP and five other true-positive metrics. For the sake of simplicity, we train object detection models using only LiDAR sensor information.

Results. After semi-supervised training, we evaluate our student model performance on the nuScenes *val* set. We compare three settings: training the student model with only the available labeled data (i.e. equivalent to teacher training), training the student model on the combination of labeled/teacher-labeled data using the naive self-training loss, and training the student model on the combination of labeled/teacher-labeled data using our proposed doubly-robust loss. We report results for training with 1/24, 1/16, and 1/4 of the total labels in Table 2. We find that the doubly-robust loss improves both mAP and NDS over using only labeled data and the naive baseline in the lower label regime, whereas performance is slightly degraded when more labels are available. Furthermore, we also show a per-class performance breakdown in Table 3. We find that the doubly robust loss consistently improves performance for both common (car, pedestrian) and rare classes. Notably, the doubly-robust loss is even able to improve upon the teacher in classes for which pseudo-label training *decreases* performance when using the naive training (e.g. barriers and traffic cones).

4 Conclusion

In this paper, we propose the new doubly-robust loss for self-training. Theoretically, we analyze the double-robustness property of the proposed loss and show its statistical efficiency when the pseudo-labels are accurate. Empirically, we see large improvements in both image classification and 3D object detection datasets. As part of future work, it would be interesting to understand how the doubly robust loss can be applied to other domains of questions, including model distillation, transfer learning, and continual learning. It is also important to find practical and efficient algorithms when the labeled and unlabeled data do not match in distribution.

References

A. N. Angelopoulos, S. Bates, C. Fannjiang, M. I. Jordan, and T. Zrnic. Prediction-powered inference. *arXiv preprint arXiv:2301.09633*, 2023.

D. Azriel, L. D. Brown, M. Sklar, R. Berk, A. Buja, and L. Zhao. Semi-supervised linear regression. *Journal of the American Statistical Association*, 117(540):2238–2251, 2022.

H. Bang and J. M. Robins. Doubly robust estimation in missing data and causal inference models. *Biometrics*, 61(4):962–973, 2005.

D. Berthelot, N. Carlini, E. D. Cubuk, A. Kurakin, K. Sohn, H. Zhang, and C. Raffel. Remixmatch: Semi-supervised learning with distribution alignment and augmentation anchoring. *arXiv preprint arXiv:1911.09785*, 2019a.

D. Berthelot, N. Carlini, I. Goodfellow, N. Papernot, A. Oliver, and C. Raffel. Mixmatch: A holistic approach to semi-supervised learning. *arXiv preprint arXiv:1905.02249*, 2019b.

J. M. Bibby, K. V. Mardia, and J. T. Kent. *Multivariate analysis*. Academic Press, 1979.

T. Birhanu, G. Molenberghs, C. Sotto, and M. G. Kenward. Doubly robust and multiple-imputation-based generalized estimating equations. *Journal of biopharmaceutical statistics*, 21(2):202–225, 2011.

H. Caesar, V. Bankiti, A. H. Lang, S. Vora, V. E. Liong, Q. Xu, A. Krishnan, Y. Pan, G. Baldan, and O. Beijbom. nuscenes: A multimodal dataset for autonomous driving. *Proceedings of the IEEE/CVF Conference on Computer Vision and Pattern Recognition*, 2020.

V. Chernozhukov, D. Chetverikov, M. Demirer, E. Duflo, C. Hansen, W. Newey, and J. Robins. Double/debiased machine learning for treatment and structural parameters, 2018a.

V. Chernozhukov, W. Newey, and R. Singh. De-biased machine learning of global and local parameters using regularized riesz representers. *arXiv preprint arXiv:1802.08667*, 2018b.

M. De Lange, R. Aljundi, M. Masana, S. Parisot, X. Jia, A. Leonardis, G. Slabaugh, and T. Tuytelaars. A continual learning survey: Defying forgetting in classification tasks. *IEEE transactions on pattern analysis and machine intelligence*, 44(7):3366–3385, 2021.

M. Ding, B. Xiao, N. Codella, P. Luo, J. Wang, and L. Yuan. Davit: Dual attention vision transformers. In *Computer Vision–ECCV 2022: 17th European Conference, Tel Aviv, Israel, October 23–27, 2022, Proceedings, Part XXIV*, pages 74–92. Springer, 2022.

P. Ding and F. Li. Causal inference. *Statistical Science*, 33(2):214–237, 2018.

D. J. Foster and V. Syrgkanis. Orthogonal statistical learning. *arXiv preprint arXiv:1901.09036*, 2019.

J. Gou, B. Yu, S. J. Maybank, and D. Tao. Knowledge distillation: A survey. *International Journal of Computer Vision*, 129:1789–1819, 2021.

K. He, X. Zhang, S. Ren, and J. Sun. Deep residual learning for image recognition. In *Proceedings of the IEEE conference on computer vision and pattern recognition*, pages 770–778, 2016.

P. W. Holland. Statistics and causal inference. *Journal of the American statistical Association*, 81 (396):945–960, 1986.

J. Jeong, S. Lee, J. Kim, and N. Kwak. Consistency-based semi-supervised learning for object detection. In *Advances in Neural Information Processing Systems*, 2019.

C. M. Jiang, M. Najibi, C. R. Qi, Y. Zhou, and D. Anguelov. Improving the intra-class long-tail in 3d detection via rare example mining. In *Computer Vision–ECCV 2022: 17th European Conference, Tel Aviv, Israel, October 23–27, 2022, Proceedings, Part X*, pages 158–175. Springer, 2022.

J. D. Kang and J. L. Schafer. Demystifying double robustness: A comparison of alternative strategies for estimating a population mean from incomplete data. 2007.

A. H. Lang, S. Vora, H. Caesar, L. Zhou, J. Yang, and O. Beijbom. Pointpillars: Fast encoders for object detection from point clouds. *Proceedings of the IEEE/CVF Conference on Computer Vision and Pattern Recognition*, pages 12689–12697, 2019.

D.-H. Lee. Pseudo-label : The simple and efficient semi-supervised learning method for deep neural networks. *ICML 2013 Workshop : Challenges in Representation Learning (WREPL)*, 07 2013.

J. Li, Z. Liu, J. Hou, and D. Liang. Dds3d: Dense pseudo-labels with dynamic threshold for semi-supervised 3d object detection. In *Proceedings of the IEEE International Conference on Robotics and Automation (ICRA)*, 2023.

T.-Y. Lin, P. Goyal, R. Girshick, K. He, and P. Dollár. Focal loss for dense object detection. In *ICCV*, pages 2980–2988, 2017.

C. Liu, C. Gao, F. Liu, P. Li, D. Meng, and X. Gao. Hierarchical supervision and shuffle data augmentation for 3d semi-supervised object detection. In *Proceedings of the IEEE/CVF Conference on Computer Vision and Pattern Recognition*, 2023.

Y.-C. Liu, C.-Y. Ma, Z. He, C.-W. Kuo, K. Chen, P. Zhang, B. Wu, Z. Kira, and P. Vajda. Unbiased teacher for semi-supervised object detection. In *Proceedings of the International Conference on Learning Representations (ICLR)*, 2021a.

Z. Liu, Y. Lin, Y. Cao, H. Hu, Y. Wei, Z. Zhang, S. Lin, and B. Guo. Swin transformer: Hierarchical vision transformer using shifted windows. In *ICCV*, 2021b.

I. Loshchilov and F. Hutter. Decoupled weight decay regularization. *arXiv preprint arXiv:1711.05101*, 2017.

A. W. Marshall and I. Olkin. Multivariate chebyshev inequalities. *The Annals of Mathematical Statistics*, pages 1001–1014, 1960.

S. J. Pan and Q. Yang. A survey on transfer learning. *IEEE Transactions on knowledge and data engineering*, 22(10):1345–1359, 2010.

J. Park, C. Xu, Y. Zhou, M. Tomizuka, and W. Zhan. Detmatch: Two teachers are better than one for joint 2d and 3d semi-supervised object detection. *Computer Vision–ECCV 2022: 17th European Conference, Tel Aviv, Israel*, 2022.

C. R. Qi, Y. Zhou, M. Najibi, P. Sun, K. Vo, B. Deng, and D. Anguelov. Offboard 3d object detection from point cloud sequences. In *Proceedings of the IEEE/CVF Conference on Computer Vision and Pattern Recognition*, 2021.

P. R. Rosenbaum and D. B. Rubin. The central role of the propensity score in observational studies for causal effects. *Biometrika*, 70(1):41–55, 1983.

D. B. Rubin. Inference and missing data. *Biometrika*, 63(3):581–592, 1976.

D. B. Rubin. Using multivariate matched sampling and regression adjustment to control bias in observational studies. *Journal of the American Statistical Association*, 74(366a):318–328, 1979.

O. Russakovsky, J. Deng, H. Su, J. Krause, S. Satheesh, S. Ma, Z. Huang, A. Karpathy, A. Khosla, M. Bernstein, et al. ImageNet large scale visual recognition challenge. *International journal of computer vision*, 115:211–252, 2015.

D. O. Scharfstein, A. Rotnitzky, and J. M. Robins. Adjusting for nonignorable drop-out using semiparametric nonresponse models. *Journal of the American Statistical Association*, 94(448): 1096–1120, 1999.

V. Semenova, M. Goldman, V. Chernozhukov, and M. Taddy. Estimation and inference on heterogeneous treatment effects in high-dimensional dynamic panels. *arXiv preprint arXiv:1712.09988*, 2017.

L. N. Smith and N. Topin. Super-convergence: Very fast training of neural networks using large learning rates. In *Artificial Intelligence and Machine Learning for Multi-Domain Operations Applications*, volume 11006, page 1100612. International Society for Optics and Photonics, 2019.

K. Sohn, D. Berthelot, C.-L. Li, Z. Zhang, N. Carlini, E. D. Cubuk, A. Kurakin, H. Zhang, and C. Raffel. Fixmatch: Simplifying semi-supervised learning with consistency and confidence. *arXiv preprint arXiv:2001.07685*, 2020a.

K. Sohn, Z. Zhang, C.-L. Li, H. Zhang, C.-Y. Lee, and T. Pfister. A simple semi-supervised learning framework for object detection. In *arXiv:2005.04757*, 2020b.

Y. Tang, W. Chen, Y. Luo, and Y. Zhang. Humble teachers teach better students for semi-supervised object detection. *2021 IEEE/CVF Conference on Computer Vision and Pattern Recognition (CVPR)*, pages 3131–3140, 2021.

H. Wang, Y. Cong, O. Litany, Y. Gao, and L. J. Guibas. 3dioumatch: Leveraging iou prediction for semi-supervised 3d object detection. In *Proceedings of the IEEE/CVF Conference on Computer Vision and Pattern Recognition*, pages 14615–14624, 2021.

K. Weiss, T. M. Khoshgoftaar, and D. Wang. A survey of transfer learning. *Journal of Big data*, 3(1): 1–40, 2016.

Q. Xie, M.-T. Luong, E. Hovy, and Q. V. Le. Self-training with noisy student improves ImageNet classification. In *Proceedings of the IEEE/CVF conference on computer vision and pattern recognition*, pages 10687–10698, 2020.

T. Yin, X. Zhou, and P. Krähenbühl. Center-based 3d object detection and tracking. *Proceedings of the IEEE/CVF Conference on Computer Vision and Pattern Recognition*, 2021.

A. Zhang, L. D. Brown, and T. T. Cai. Semi-supervised inference: General theory and estimation of means. 2019.

H. Zhou, Z. Ge, S. Liu, W. Mao, Z. Li, H. Yu, and J. Sun. Dense teacher: Dense pseudo-labels for semi-supervised object detection. In S. Avidan, G. Brostow, M. Cissé, G. M. Farinella, and T. Hassner, editors, *Computer Vision – ECCV 2022*, pages 35–50, 2022.

B. Zhu, Z. Jiang, X. Zhou, Z. Li, and G. Yu. Class-balanced grouping and sampling for point cloud 3d object detection. *arXiv preprint arXiv:1908.09492*, 2019.

X. J. Zhu. Semi-supervised learning literature survey. 2005.

A Implementation Details of Image Classification

We evaluate our doubly-robust self-training on the ImageNet100 and mini-ImageNet100 datasets, which are subsets of ImageNet-1k from ImageNet Large Scale Visual Recognition Challenge 2012 (Russakovsky et al., 2015). Two models are evaluated: **1)** DaViT-T (Ding et al., 2022), a state-of-the-art 12-layer vision transformer architecture with a patch size of 4, a window size of 7, and an embedding dim of 768, and **2)** ResNet50 (He et al., 2016), a classic and powerful convolutional network with 50 layers and embedding dim 2048. We evaluate all the models on the same ImageNet100 validation set (50 samples per class). For the training, we use the same data augmentation and regularization strategies following the common practice in Liu et al. (2021b); Lin et al. (2017); Ding et al. (2022). We train all the models with a batch size of 1024 on 8 Tesla V100 GPUs (the batch size is reduced to 64 if the number of training data is less than 1000). We use AdamW (Loshchilov and Hutter, 2017) optimizer and a simple triangular learning rate schedule (Smith and Topin, 2019). The weight decay is set to 0.05 and the maximal gradient norm is clipped to 1.0. The stochastic depth drop rates are set to 0.1 for all models. During training, we crop images randomly to 224×224, while a center crop is used during evaluation on the validation set. We use a curriculum setting where the α_t grows linearly or quadratically from 0 to 1 throughout the training. To show the effectiveness of our method, we also compare model training with different curriculum learning settings and varying numbers of epochs.

B Ablative Experiments on Image Classification

Table 4: Ablation study on different curriculum settings on ImageNet-100. All models are trained in 20 epochs.

Methods	30% GTs		50% GTs		70% GTs		90% GTs	
	top1	top5	top1	top5	top1	top5	top1	top5
Naive Labeled + Pseudo	28.01	54.63	37.6	66.72	43.76	73.42	47.74	77.15
Doubly-Robust, $\alpha_t = 1$	28.43	56.65	38.06	67.18	43.22	73.18	48.52	77.21
Doubly-Robust, $\alpha_t = t/T$ (linear)	30.87	60.98	40.18	71.06	**46.60**	**75.80**	**50.44**	**78.88**
Doubly-Robust, $\alpha_t = (t/T)^2$ (quadratic)	**31.15**	**61.29**	**40.86**	**71.14**	45.50	75.11	49.64	77.77

Ablation Study on Curriculum Settings. There are three options for the curriculum setting: 1) $\alpha_t = 1$ throughout the whole training, 2) grows linearly with training iterations $\alpha_t = t/T$, 3) grows quadratically with training iterations $\alpha_t = (t/T)^2$. From results in Table 4, we see: the first option achieves comparable performance with the 'Naive Labeled + Pseudo' baseline. Both the linear and quadratic strategies show significant performance improvements: the linear one works better when more labeled data is available, e.g., 70% and 90%, while the quadratic one prefers less labeled data, e.g. 30% and 50%.

Table 5: Ablation study on the number of epochs. All models are trained using 10% labeled data on ImageNet-100.

Training epochs	Labeled Only		Pseudo Only		Labeled + Pseudo		Doubly-Robust Loss	
	top1	top5	top1	top5	top1	top5	top1	top5
20	16.02	39.68	17.02	38.64	19.38	41.96	**21.88**	**47.18**
50	25.00	51.21	28.90	53.74	30.36	57.04	**36.65**	**65.68**
100	35.57	64.66	44.43	**71.56**	42.44	68.94	**45.98**	70.66

Ablation Study on the Number of Epochs. We conduct experiments on different training epochs. The results are shown in Table 5. Our model is consistently superior to the baselines. And we can observe the gain is larger when the number of training epochs is relatively small, e.g. 20 and 50.

C Implementation Details of 3D Object Detection

Our experiments follow the standard approach for semi-supervised detection: we first initialize two detectors, the teacher (i.e. labeler) and the student. First, a random split of varying sizes is selected

from the nuScenes training set. We pre-train the teacher network using the ground-truth annotations in this split. Following this, we freeze the weights in the teacher model and then use it to generate pseudo-labels on the entire training set. The student network is then trained on a combination of the pseudo-labels and ground-truth labels originating from the original split. In all of our semi-supervised experiments, we use CenterPoint with a PointPillars backbone as our 3D detection model (Yin et al., 2021; Lang et al., 2019). The teacher pre-training and student training are both conducted for 10 epochs on 3 NVIDIA RTX A6000 GPUs. We follow the standard nuScenes training setting outlined in Zhu et al. (2019), with the exception of disabling ground-truth paste augmentation during training to prevent data leakage from the labeled split. To select the pseudo-labels to be used in training the student, we simply filter the teacher predictions by detection confidence, using all detections above a chosen threshold. We use a threshold of 0.3 for all classes, as in Park et al. (2022). In order to conduct training in a batch-wise manner, we compute the loss over only the samples contained within the batch. We construct each batch to have a consistent ratio of labeled/unlabeled samples to ensure the loss is well-defined for the batch.

D Discussions when $\hat{f}$ is trained from labeled data

In Theorem 2, we analyze the double robustness of the proposed loss function when the predictor $\hat{f}$ is pre-existing and not trained from the labeled dataset. In practice, one may only have access to the labeled and unlabeled dataset without a pre-existing teacher model. In this case, one may choose to split the labeled samples $\mathcal{D}_2$ into two parts. The last $n/2$ samples are used to train $\hat{f}$, and the first $n/2$ samples are used in the doubly-robust loss:

$$\mathcal{L}^{\mathsf{DR2}}_{\mathcal{D}_1,\mathcal{D}_2}(\theta) = \frac{1}{m}\sum_{i=1}^{m}\ell_\theta(X_i,\hat{f}(X_i)) - \frac{2}{n}\sum_{i=m+1}^{m+n/2}\frac{1}{\pi(X_i)}\ell_\theta(X_i,\hat{f}(X_i)) + \frac{2}{n}\sum_{i=m+1}^{m+n/2}\frac{1}{\pi(X_i)}\ell_\theta(X_i,Y_i).$$

Since $\hat{f}$ is independent of all samples used in the above loss, the result in Theorem 2 continues to hold. Asymptotically, such doubly-robust estimator is always no worse than the estimator trained only on the labeled data.

E Proof of Proposition 1

For the labeled-only estimator $\hat{\theta}_{\mathsf{TL}}$, we have

$$\mathbb{E}[(\theta^\star - \hat{\theta}_{\mathsf{TL}})^2] = \mathbb{E}\left[\left(\mathbb{E}[Y] - \frac{1}{n}\sum_{i=m+1}^{m+n} Y\right)^2\right] = \frac{1}{n}\mathsf{Var}[Y].$$

For the self-training loss, we have

$$\begin{aligned}
\mathbb{E}[(\theta^\star - \hat{\theta}_{\mathsf{SL}})^2] &= \mathbb{E}\left[\left(\mathbb{E}[Y] - \frac{1}{m+n}\left(\sum_{i=1}^{m}\hat{f}(X_i) + \sum_{i=m+1}^{m+n} Y_i\right)\right)^2\right] \\
&\le 2\left(\mathbb{E}\left[\left(\frac{m}{m+n}\left(\mathbb{E}[Y] - \frac{1}{m}\sum_{i=1}^{m}\hat{f}(X_i)\right)\right)^2\right] + \mathbb{E}\left[\left(\frac{n}{m+n}\left(\mathbb{E}[Y] - \frac{1}{n}\sum_{i=m+1}^{m+n} Y_i\right)\right)^2\right]\right) \\
&\le \frac{2m^2}{(m+n)^2}\mathbb{E}[(\hat{f}(X)-Y)]^2 + \frac{2m}{(m+n)^2}\mathsf{Var}[\hat{f}(X)-Y] + \frac{2n}{(m+n)^2}\mathsf{Var}[Y].
\end{aligned}$$

For the doubly robust loss, on one hand, we have

$$\begin{aligned}
\mathbb{E}[(\theta^\star - \hat{\theta}_{\mathsf{DR}})^2] &= \mathbb{E}\left[\left(\mathbb{E}[Y] - \frac{1}{m+n}\sum_{i=1}^{m+n}\hat{f}(X_i) + \frac{1}{n}\sum_{i=m+1}^{m+n}(\hat{f}(X_i) - Y_i)\right)^2\right] \\
&\le 2\mathbb{E}\left[\left(\mathbb{E}[Y] - \frac{1}{n}\sum_{i=m+1}^{m+n} Y_i\right)^2\right] + 2\mathbb{E}\left[\left(\mathbb{E}[\hat{f}(X)] - \frac{1}{n}\sum_{i=m+1}^{m+n}\hat{f}(X_i)\right)^2\right] \\
&\quad + 2\mathbb{E}\left[\left(\mathbb{E}[\hat{f}(X)] - \frac{1}{m+n}\sum_{i=1}^{m+n}\hat{f}(X_i)\right)^2\right] \\
&= \frac{2}{n}\mathsf{Var}[Y] + \left(\frac{2}{m+n} + \frac{2}{n}\right)\mathsf{Var}[\hat{f}(X)].
\end{aligned}$$

On the other hand, we have

$$\begin{aligned}
\mathbb{E}[(\theta^\star - \hat{\theta}_{\mathsf{DR}})^2] &= \mathbb{E}\left[\left(\mathbb{E}[Y] - \frac{1}{m+n}\sum_{i=1}^{m+n}\hat{f}(X_i) + \frac{1}{n}\sum_{i=m+1}^{m+n}(\hat{f}(X_i) - Y_i)\right)^2\right] \\
&\le 2\mathbb{E}\left[\left(\mathbb{E}[Y] - \frac{1}{m+n}\sum_{i=1}^{m+n} Y_i\right)^2\right] + 2\mathbb{E}\left[\left(\mathbb{E}[\hat{f}(X) - Y] - \frac{1}{n}\sum_{i=m+1}^{m+n}(\hat{f}(X_i) - Y_i)\right)^2\right] \\
&\quad + 2\mathbb{E}\left[\left(\mathbb{E}[\hat{f}(X) - Y] - \frac{1}{m+n}\sum_{i=1}^{m+n}(\hat{f}(X_i) - Y_i)\right)^2\right] \\
&= \left(\frac{2}{m+n} + \frac{2}{n}\right)\mathsf{Var}[\hat{f}(X) - Y] + \frac{2}{m+n}\mathsf{Var}[Y].
\end{aligned}$$

The proof is done by taking the minimum of the two upper bounds.

F Proof of Theorem 2

Proof. We know that

$$\begin{aligned}
&\|\nabla_\theta \mathcal{L}^{\mathsf{DR}}_{\mathcal{D}_1,\mathcal{D}_2}(\theta^\star) - \mathbb{E}[\nabla_\theta \mathcal{L}^{\mathsf{DR}}_{\mathcal{D}_1,\mathcal{D}_2}(\theta^\star)]\|_2 \\
=&\Big\|\frac{1}{m+n}\sum_{i=1}^{m+n}(\nabla_\theta \ell_{\theta^\star}(X_i, \hat{f}(X_i)) - \mathbb{E}[\nabla_\theta \ell_{\theta^\star}(X, \hat{f}(X))]) + \frac{1}{n}\sum_{i=m+1}^{m+n}\Big(\nabla_\theta \ell_{\theta^\star}(X_i, Y_i) - \nabla_\theta \ell_{\theta^\star}(X_i, \hat{f}(X_i)) \\
&- \mathbb{E}[\nabla_\theta \ell_{\theta^\star}(X, Y) - \nabla_\theta \ell_{\theta^\star}(X, \hat{f}(X))]\Big)\Big\|_2 \\
\le&\Big\|\frac{1}{m+n}\sum_{i=1}^{m+n}(\nabla_\theta \ell_{\theta^\star}(X_i, \hat{f}(X_i)) - \mathbb{E}[\nabla_\theta \ell_{\theta^\star}(X, \hat{f}(X))])\Big\|_2 + \Big\|\frac{1}{n}\sum_{i=m+1}^{m+n}\Big(\nabla_\theta \ell_{\theta^\star}(X_i, Y_i) - \nabla_\theta \ell_{\theta^\star}(X_i, \hat{f}(X_i)) \\
&- \mathbb{E}[\nabla_\theta \ell_{\theta^\star}(X, Y) - \nabla_\theta \ell_{\theta^\star}(X, \hat{f}(X))]\Big)\Big\|_2.
\end{aligned}$$

From the multi-dimensional Chebyhshev's inequality (Bibby et al., 1979; Marshall and Olkin, 1960), we have with probability at least $1 - \delta/2$, for some universal constant C,

$$\Big\|\frac{1}{m+n}\sum_{i=1}^{m+n}(\nabla_\theta \ell_{\theta^\star}(X_i, \hat{f}(X_i)) - \mathbb{E}[\nabla_\theta \ell_{\theta^\star}(X, \hat{f}(X))])\Big\|_2 \le C\|\Sigma^{\hat{f}}_{\theta^\star}\|_2\sqrt{\frac{d}{(m+n)\delta}}.$$

Similarly, we also have with probability at least $1 - \delta/2$,

$$\Big\|\frac{1}{n}\sum_{i=m+1}^{m+n}\Big(\nabla_\theta \ell_{\theta^\star}(X_i, Y_i) - \nabla_\theta \ell_{\theta^\star}(X_i, \hat{f}(X_i)) - \mathbb{E}[\nabla_\theta \ell_{\theta^\star}(X, Y) - \nabla_\theta \ell_{\theta^\star}(X, \hat{f}(X))]\Big)\Big\|_2 \le C\|\Sigma^{Y-\hat{f}}_{\theta^\star}\|_2\sqrt{\frac{d}{n\delta}}.$$

Furthermore, note that

$$\mathbb{E}[\nabla_\theta \mathcal{L}^{\mathsf{DR}}_{\mathcal{D}_1,\mathcal{D}_2}(\theta^\star)] = \mathbb{E}[\nabla_\theta \ell_{\theta^\star}(X,Y)] = \nabla_\theta \mathbb{E}[\ell_{\theta^\star}(X,Y)] = 0.$$

Here we use Assumption 1 and Assumption 2 to ensure that the expectation and differentiation are interchangeable. Thus we have with probability at least $1-\delta$,

$$\|\nabla_\theta \mathcal{L}^{\mathsf{DR}}_{\mathcal{D}_1,\mathcal{D}_2}(\theta^\star)\|_2 \le C\left(\|\Sigma^{\hat{f}}_{\theta^\star}\|_2\sqrt{\frac{d}{(m+n)\delta}} + \|\Sigma^{Y-\hat{f}}_{\theta^\star}\|_2\sqrt{\frac{d}{n\delta}}\right).$$

On the other hand, we can also write the difference as

$$\begin{aligned}
&\|\nabla_\theta \mathcal{L}^{\mathsf{DR}}_{\mathcal{D}_1,\mathcal{D}_2}(\theta^\star) - \mathbb{E}[\nabla_\theta \mathcal{L}^{\mathsf{DR}}_{\mathcal{D}_1,\mathcal{D}_2}(\theta^\star)]\|_2 \\
=&\Big\|\frac{1}{m+n}\sum_{i=1}^{m+n}(\nabla_\theta \ell_{\theta^\star}(X_i,\hat{f}(X_i)) - \mathbb{E}[\nabla_\theta \ell_{\theta^\star}(X,\hat{f}(X))]) + \frac{1}{n}\sum_{i=m+1}^{m+n}\Big(\nabla_\theta \ell_{\theta^\star}(X_i,Y_i) - \mathbb{E}[\nabla_\theta \ell_{\theta^\star}(X,Y)]\Big) \\
&- \frac{1}{n}\sum_{i=m+1}^{m+n}\Big(\nabla_\theta \ell_{\theta^\star}(X_i,Y_i) - \mathbb{E}[\nabla_\theta \ell_{\theta^\star}(X,\hat{f}(X))]\Big)\Big\|_2 \\
\le&\Big\|\frac{1}{m+n}\sum_{i=1}^{m+n}(\nabla_\theta \ell_{\theta^\star}(X_i,\hat{f}(X_i)) - \mathbb{E}[\nabla_\theta \ell_{\theta^\star}(X,\hat{f}(X))])\Big\|_2 + \Big\|\frac{1}{n}\sum_{i=m+1}^{m+n}\Big(\nabla_\theta \ell_{\theta^\star}(X_i,Y_i) - \mathbb{E}[\nabla_\theta \ell_{\theta^\star}(X,Y)]\Big)\Big\|_2 \\
&+ \Big\|\frac{1}{n}\sum_{i=m+1}^{m+n}\Big(\nabla_\theta \ell_{\theta^\star}(X_i,Y_i) - \mathbb{E}[\nabla_\theta \ell_{\theta^\star}(X,\hat{f}(X))]\Big)\Big\|_2 \\
\le&C\left(\|\Sigma^{\hat{f}}_{\theta^\star}\|_2\left(\sqrt{\frac{d}{(m+n)\delta}} + \sqrt{\frac{d}{n\delta}}\right) + \|\Sigma^{Y}_{\theta^\star}\|_2\sqrt{\frac{d}{n\delta}}\right).
\end{aligned}$$

Here the last inequality uses multi-dimensional Chebyshev's inequality and holds with probability at least $1-\delta$. This finishes the proof. □

G Proof of Proposition 3

Proof. We have

$$\begin{aligned}
\mathbb{E}[\mathcal{L}^{\mathsf{DR2}}_{\mathcal{D}_1,\mathcal{D}_2}(\theta)] =& \frac{1}{m}\sum_{i=1}^{m}\mathbb{E}_{X_i\sim\mathbb{P}_X}[\ell_\theta(X_i,\hat{f}(X_i))] - \frac{1}{n}\sum_{i=m+1}^{m+n}\mathbb{E}_{X_i\sim\mathbb{Q}_X}\left[\frac{1}{\pi(X_i)}\ell_\theta(X_i,\hat{f}(X_i))\right] \\
&+ \frac{1}{n}\sum_{i=m+1}^{m+n}\mathbb{E}_{X_i\sim\mathbb{Q}_X,Y_i\sim\mathbb{P}_{Y|X_i}}\left[\frac{1}{\pi(X_i)}\ell_\theta(X_i,Y_i)\right] \\
=& \mathbb{E}_{X\sim\mathbb{P}_X}[\ell_\theta(X,\hat{f}(X))] - \mathbb{E}_{X\sim\mathbb{Q}_X}\left[\frac{1}{\pi(X)}\ell_\theta(X,\hat{f}(X))\right] \\
&+ \mathbb{E}_{X\sim\mathbb{Q}_X,Y\sim\mathbb{P}_{Y|X}}\left[\frac{1}{\pi(X)}\ell_\theta(X,Y)\right].
\end{aligned}$$

In the first case when $\pi(x) \equiv \frac{\mathbb{P}_X(x)}{\mathbb{Q}_X(x)}$, we have

$$\begin{aligned}
\mathbb{E}[\mathcal{L}^{\mathsf{DR2}}_{\mathcal{D}_1,\mathcal{D}_2}(\theta)] =& \mathbb{E}_{X\sim\mathbb{P}_X}[\ell_\theta(X,\hat{f}(X))] - \mathbb{E}_{X\sim\mathbb{Q}_X}\left[\frac{\mathbb{P}_X(X)}{\mathbb{Q}_X(X)}\ell_\theta(X,\hat{f}(X))\right] \\
&+ \mathbb{E}_{X\sim\mathbb{Q}_X,Y\sim\mathbb{P}_{Y|X}}\left[\frac{\mathbb{P}_X(X)}{\mathbb{Q}_X(X)}\ell_\theta(X,Y)\right] \\
=& \mathbb{E}_{X\sim\mathbb{P}_X}[\ell_\theta(X,\hat{f}(X))] - \mathbb{E}_{X\sim\mathbb{P}_X}\left[\ell_\theta(X,\hat{f}(X))\right] \\
&+ \mathbb{E}_{X\sim\mathbb{P}_X,Y\sim\mathbb{P}_{Y|X}}[\ell_\theta(X,Y)] \\
=& \mathbb{E}_{X,Y\sim\mathbb{P}_{X,Y}}[\ell_\theta(X,Y)].
\end{aligned}$$

In the second case when $\ell_\theta(x, \hat{f}(x)) = \mathbb{E}_{Y\sim\mathbb{P}_{Y|X=x}}[\ell_\theta(x, Y)]$, we have

$$\begin{aligned}
\mathbb{E}[\mathcal{L}^{\mathsf{DR2}}_{\mathcal{D}_1,\mathcal{D}_2}(\theta)] &= \mathbb{E}_{X\sim\mathbb{P}_X}[\ell_\theta(X, \hat{f}(X))] - \mathbb{E}_{X\sim\mathbb{Q}_X}\left[\frac{1}{\pi(X)}\ell_\theta(X, \hat{f}(X))\right] \\
&\quad + \mathbb{E}_{X\sim\mathbb{Q}_X}\mathbb{E}_{Y\sim\mathbb{P}_{Y|X}}\left[\frac{1}{\pi(X)}\ell_\theta(X, Y) \mid X\right] \\
&= \mathbb{E}_{X\sim\mathbb{P}_X}[\ell_\theta(X, \hat{f}(X))] - \mathbb{E}_{X\sim\mathbb{Q}_X}\left[\frac{1}{\pi(X)}\ell_\theta(X, \hat{f}(X))\right] \\
&\quad + \mathbb{E}_{X\sim\mathbb{Q}_X}\left[\frac{1}{\pi(X)}\ell_\theta(X, \hat{f}(X))\right] \\
&= \mathbb{E}_{X\sim\mathbb{P}_X}[\ell_\theta(X, \hat{f}(X))] \\
&= \mathbb{E}_{X,Y\sim\mathbb{P}_{X,Y}}\left[\ell_\theta(X, Y)\right].
\end{aligned}$$

This finishes the proof. □